Inorg. Chem. **2005**, *44*, 2039–2049

Structural Determination of Ruthenium–Porphyrin Complexes Relevant to Catalytic Epoxidation of Olefins

Emma Gallo,[†] Alessandro Caselli,[†] Fabio Ragaini,[†] Simone Fantauzzi,[†] Norberto Masciocchi,[‡] Angelo Sironi,[§] and Sergio Cenini*,[†]

Dipartimento di Chimica Inorganica, Metallorganica e Analitica, Università di Milano, and ISTM-CNR, Via Venezian 21, 20133 Milano, Italy, Dipartimento di Scienze Chimiche ed Ambientali, Università dell'Insubria, Via Valleggio 11, 22100 Como, Italy, and Dipartimento di Chimica Strutturale e Stereochimica Inorganica, Università di Milano, and ISTM-CNR, Via Venezian 21, 20133 Milano, Italy

Received October 8, 2004

A reproducible synthesis of a competent epoxidation catalyst, $[Ru^{VI}(TPP)(O)_2]$ (TPP = tetraphenylporphyrin dianion), starting from $[Ru^{II}(TPP)(CO)L]$ (L = none or CH_3OH), is described. The molecular structure of the complex was determined by using ab initio X-ray powder diffraction (XRPD) methods, and its solution behavior was in detail investigated by NMR techniques such as PGSE (pulsed field gradient spin-echo) measurements. $[Ru^{IV}(TPP)(OH)]_2O$, a reported byproduct in the synthesis of $[Ru^{VI}(TPP)(O)_2]$, was synthesized in a pure form by oxidation of $[Ru^{II}(TPP)(CO)L]$ or by a coproportionation reaction of $[Ru^{VI}(TPP)(O)_2]$ and $[Ru^{II}(TPP)(CO)L]$, and its molecular structure was then determined by XRPD analysis. $[Ru^{VI}(TPP)(O)_2]$ can be reduced by dimethyl sulfoxide or by carbon monoxide to yield $[Ru^{II}(TPP)(S\text{-}DMSO)_2]$ or $[Ru^{II}(TPP)(CO)(H_2O)]$, respectively. These two species were characterized by conventional single-crystal X-ray diffraction analysis.

Introduction

Oxidation chemistry at metalloporphyrin centers occupies a prominent role in current research in the field of chemical and biological catalysis.[1] Among the many known species, interest in ruthenium porphyrins[2] originally stemmed, at least in part, from attempts to model certain aspects of cytochrome P450 systems.[3] In the past two decades, much progress has been achieved in the development of new generations of synthetic metalloporphyrins which are able to reproduce and mimic all the different heme−enzyme-mediated reactions such as oxygenation, oxidation, oxidative chlorination, and dismutation.[1c,2] Among oxidation reactions catalyzed by transition metal complexes, epoxidation of olefins is still one of the most attractive and is largely used in organic synthesis:[4] in a single step, two C−O bonds are created with high regio- and/or stereoselectivity control.[5] The transition metal-catalyzed epoxidation of olefins by alkyl hydroperoxides is currently performed on an industrial scale, i.e., the propene epoxidation with ^{t}BuOOH and a molybdenum-based catalyst (the Halcon process)[6] or the production of fine chemicals by the Sharpless reaction.[5b]

Metalloporphyrin-catalyzed alkene epoxidation reactions are often characterized by remarkable regio- and stereose-

* To whom correspondence should be addressed. E-mail: Sergio.Cenini@unimi.it. Fax: (+39) 02−50314405.

[†] Dipartimento di Chimica Inorganica, Metallorganica e Analitica, Università di Milano, and ISTM-CNR.

[‡] Università dell'Insubria.

[§] Dipartimento di Chimica Strutturale e Stereochimica Inorganica, Università di Milano, and ISTM-CNR.

(1) (a) Meunier, B. *Chem. Rev.* **1992**, *92*, 1411−1456. (b) Montanari, F., Casella, L., Eds. *Metalloporphyrins Catalysed Oxidations*; Kluwer Academic: Dordrecht, The Netherlands, 1994. (c) Sono, M.; Roach, M. P.; Coulter, E. D.; Dawson, J. H. *Chem. Rev.* **1996**, *96*, 2841−2887. (d) McLain, J. L.; Lee, J.; Groves, J. T. In *Biomimetic Oxidations Catalyzed by Transition Metal Complexes*; Meunier, B., Ed.; Imperial College Press: London, 2000; pp 91−169. (e) Groves, J. T.; Shalayev, K.; Lee, J. Biochemistry and Binding: Activation of Small Molecules. In *The Porphyrin Handbook*; Kadish, K. M., Smith, K. M., Guilard, R., Eds.; Academic Press: New York, 2000; Vol. 4, pp 17−40.

(2) Ezhova, M. B.; James, B. R. In *Advances in Catalytic Activation of Dioxygen by Metal Complexes*; Simandi, L., Ed.; Kluwer Academic: Dordrecht, The Netherlands, 2002; pp 1−77.

(3) Ortiz de Montellano, P. R., Ed. *Cytochrome P450: Structures, Mechanism and Biochemistry*; Plenum: New York, 1995.

(4) (a) Jorgensen, K. A. *Chem. Rev.* **1989**, *89*, 431−458. (b) Arends, I. W. C. E.; Sheldon, R. A. *Top. Catal.* **2002**, *19*, 133−141.

(5) (a) Hanson, R. M. *Chem. Rev.* **1991**, *91*, 437−476. (b) Johnson, R. A.; Sharpless, K. B. In *Catalytic Asymmetric Synthesis*; Ojima, I., Ed.; VCH: Weinheim, Germany, 1993; pp 103−158.

(6) Sheldon, R. *Bull. Soc. Chim. Belg.* **1985**, *94*, 651−670.

10.1021/ic048587w CCC: $30.25
Published on Web 02/15/2005

Scheme 1. Reported Mechanism for the Reaction of Molecular Oxygen with Ruthenium Porphyrins[14]

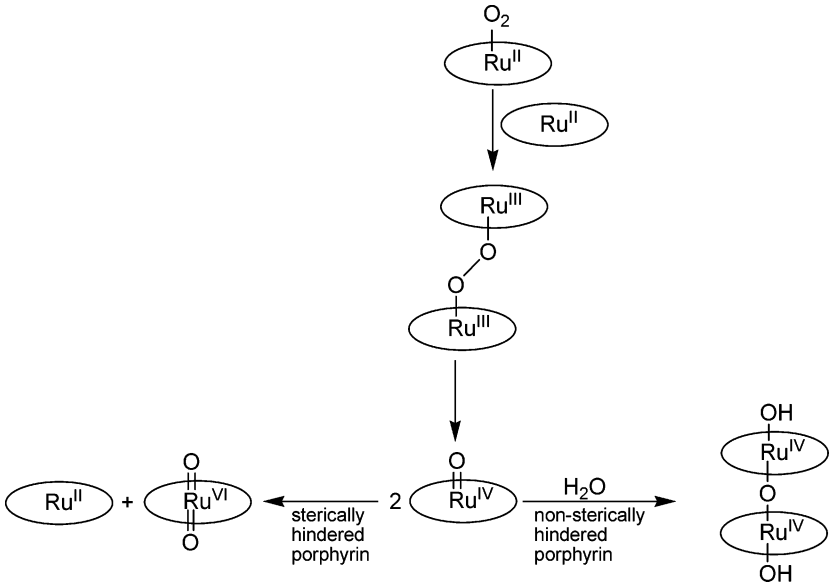

lectivities. A breakthrough in the field is the set of results achieved in 1985 by Groves and Quinn in the aerobic epoxidation of olefins catalyzed by $[Ru^{VI}(TMP)(O)_2]$ [TMP = tetrakis(2,4,6-trimethylphenyl)porphyrin dianion] at room temperature and ambient pressure.[7] Since then, several high valent dioxoruthenium(VI) porphyrin complexes have been isolated and found to be excellent catalysts for hydrocarbon oxidation.[8] Only in one case has a Ru(porphyrin)$(O)_2$ complex been structurally characterized.[8c] Systematic structural variation of the porphyrin ligand has proved to be a useful strategy for achieving electronic and steric tuning of the catalyst. Nevertheless, the structure−reactivity relationship of oxometalloporphyrin complexes remains less understood,[2] and little is known about possible deactivation routes of the catalyst.[9]

In the proposed and generally accepted mechanism, $[Ru^{VI}$(porphyrin)$(O)_2]$ transfers one oxygen atom to the olefinic substrate and the resulting monooxoruthenium complex, $[Ru^{IV}$(porphyrin)(O)], disproportionates into the epoxidizing agent, $[Ru^{VI}$(porphyrin)$(O)_2]$, and $[Ru^{II}$(porphyrin)]; the latter is in turn reoxidized and re-enters the catalytic cycle.[7b] The elusive $[Ru^{IV}(TMP)(O)]$ has been spectroscopically observed for the first time during the oxidation reaction of $[Ru^{II}(TMP)(CH_3CN)_2]$,[10] and since then, a few $[(L)Ru^{IV}$(porphyrin)(O)] species have been isolated and/or characterized (L = EtOH, THF, or $OPPh_3$).[11] Thus, the chemistry of ruthenium dioxoporphyrin complexes continues to attract much attention, despite the fact that it has been shown in recent years that when 2,6-dichloropyridine *N*-oxide is employed as the oxidant in place of dioxygen, the catalytically active species are ruthenium(V) porphyrin oxo complexes, instead of ruthenium(VI) species.[12,13] In this context, a distinction must be made between complexes of sterically hindered porphyrin dianions such as TMP and those of nonsterically demanding ones such as octaethylporphyrin dianion (OEP) and tetraphenylporphyrin dianion (TPP). Collman et al.[14] proposed a mechanism for the reaction of molecular oxygen with ruthenium porphyrins, which is outlined in Scheme 1. After reaction of dioxygen with a Ru^{II}(porphyrin) molecule, the dioxygen adduct so formed reacts with a second Ru^{II}(porphyrin) molecule leading to a μ-peroxo dimer. Homolytic cleavage of the O−O bond then leads to the formation of two unstable $[Ru^{IV}$-

(7) (a) Groves, J. T.; Quinn, R. *Inorg. Chem*. **1984**, *23*, 3844−3846. (b) Groves, J. T.; Quinn, R. *J. Am. Chem. Soc.* **1985**, *107*, 5790−5792.

(8) Selected examples: (a) Leung, W.-H.; Che, C.-M.; Yeung, C.-H.; Poon, C.-K. *Polyhedron* **1993**, *12*, 2331−2334. (b) Liu, C.-J.; Yu, W.-Y.; Peng, S.-M.; Mark, T. C. W.; Che, C.-M. *J. Chem. Soc., Dalton Trans.* **1998**, 805−812. (c) Lai, T.-S.; Zhang, R.; Cheung, K.-K.; Kwong, H.-L.; Che, C.-M. *Chem. Commun.* **1998**, 1583−1584. (d) Liu, C.-J.; Yu, W.-Y.; Che, C.-M.; Yeung, C.-H. *J. Org. Chem.* **1999**, *64*, 7365−7374. (e) Zhang, R.; Yu, W.-Y.; Lai, T.-S.; Che, C.-M. *Chem. Commun.* **1999**, 409−410. (f) Zhang, R.; Yu, W.-Y.; Sun, H.-Z.; Liu, W.-S.; Che, C.-M. *Chem.—Eur. J.* **2002**, *8*, 2495−2507. (g) Tavarès, M.; Ramasseul, R.; Marchon, J.-C.; Vallée-Goyet, D.; Gramain, J.-C. *J. Chem. Res., Synop.* **1994**, 74.

(9) (a)Scharbert, B.; Zeisberger, E.; Paulus, E. *J. Organomet. Chem.* **1995**, *493*, 143−147. (b) Cunningham, I. D.; Danks, T. N.; Hay, J. N.; Hamerton, I.; Gunathilagan, S.; Janczak, C. *J. Mol. Catal. A: Chem.* **2002**, *185*, 25−31.

(10) Groves, J. T.; Ahn, K.-H. *Inorg. Chem*. **1987**, *26*, 3831−3833.

(11) (a) Leung, W.-H.; Che, C.-M. *J. Am. Chem. Soc*. **1989**, *111*, 8812−8818. (b) Groves, J. T.; Roman, J. S. *J. Am. Chem. Soc*. **1995**, *117*, 5594−5595. (c) Bailey, A. J.; James, B. R. *Chem. Commun*. **1996**, 2343−2344. (d) Cheng, S. Y. S.; James, B. R. *J. Mol. Catal. A: Chem.* **1997**, *117*, 91−102.

(12) Sharma, P. K.; de Visser, S. P.; Ogliaro, F.; Shaik, S. *J. Am. Chem. Soc*. **2003**, *125*, 2291−2300.

(13) (a) Ohtake, H.; Higushi, T.; Hirobe, M. *Tetrahedron Lett.* **1992**, *33*, 2521−2524. (b) Ohtake, H.; Higushi, T.; Hirobe, M. *J. Am. Chem. Soc*. **1992**, *114*, 10660−10662. (c) Ohtake, H.; Higuchi, T.; Hirobe, M. *Heterocycles* **1995**, *40*, 867−903. (d) Higuchi, T.; Hirobe, M. *J. Mol. Catal. A: Chem.* **1996**, *113*, 403−422. (e) Groves, J. T.; Bonchio, M.; Carofiglio, T.; Shalyaev, K. *J. Am. Chem. Soc*. **1996**, *118*, 8961−8962. (f) Gross, Z.; Ini, S.; Kapon, M.; Cohen, S. *Tetrahedron Lett.* **1996**, *37*, 7325−7328. (g) Gross, Z.; Ini, S. *J. Org. Chem.* **1997**, *62*, 5514−5521. (h) Gross, Z.; Ini, S. *Inorg. Chem.* **1999**, *38*, 1446−1449. (i) Zhang, R.; Yu, W.-Y.; Wong, K.-Y.; Che, C.-M. *J. Org. Chem.* **2001**, *66*, 8145−8153. (j) Le Maux, P.; Lukas, M.; Simonneaux, G. *J. Mol. Catal. A: Chem.* **2003**, *206*, 95−103.

(14) (a) Collman, J. P.; Barnes, C. E.; Brothers, P. J.; Collins, T. J.; Ozawa, T.; Gallucci, J. C.; Ibers, J. A. *J. Am. Chem. Soc*. **1984**, *106*, 5151−5163. (b) Collman, J. P.; Brauman, J. I.; Fitgerald, J. P.; Sparanpany, J. W.; Ibers, J. A. *J. Am. Chem. Soc.* **1988**, *110*, 3486-3495.

Chart 1. Ruthenium Tetraphenylporphyrinate Complexes

$[Ru^{II}(TPP)(CO)]$	(**1**)	$[Ru^{IV}(TPP)(OH)]_2(O)$	(**4**)
$[Ru^{II}(TPP)(CO)(CH_3OH)]$	(**2**)	$[Ru^{II}(TPP)(S\text{-}DMSO)_2]$	(**5**)
$[Ru^{VI}(TPP)(O)_2]$	(**3**)	$[Ru^{II}(TPP)(CO)(H_2O)]$	(**6**)

(porphyrin)(O)] complexes. Depending on the steric properties of the porphyrin, either a *trans*-dioxo-Ru^{VI}(porphyrin) complex (through disproportionation) or a μ-oxo-Ru^{IV}-(porphyrin) dimer is formed, by formal addition of a water molecule (Scheme 1).

In addition to the steric properties of the porphyrin, the solvent also plays a key role in driving the reaction in one direction or the other. Indeed, it has been shown that it is possible to obtain *trans*-dioxo complexes of nonsterically hindered porphyrins such as $TPPH_2$ and $OEPH_2$ by chemical oxidation with *m*-CPBA (*m*-chloroperoxybenzoic acid) of the starting carbonyls when working in the presence of weak coordinating solvents such as alcohols.[11a,15]

Since the early work of Masuda and co-authors,[16] several independent syntheses of $[Ru^{IV}(porphyrin)(OH)]_2(O)$ complexes have been reported.[17] Despite these extensive investigations, very little is known about the possible pathways leading to these catalytically inert μ-oxo-Ru^{IV}(porphyrin) dimers under the conditions employed in catalysis or about the exact role played by the solvent or by the oxidant (in its pristine or reduced forms).

Our interest has been focused on the synthesis and structural characterization of the highly reactive $[Ru^{VI}(TPP)(O)_2]$ species. Several previously published papers deal with the synthesis of *trans*-dioxo complexes of nonsterically hindered porphyrins, mainly employing $[Ru^{II}(porphyrin)(CO)(MeOH)]$ as the starting material and carrying out the oxidation with oxidants such as *m*-CPBA, TBHP (*tert*-butylhydroperoxide), or PhIO.[11a,15,18] In our hands and in the case of TPP as the porphyrin, however, none of the published methods showed a good reproducibility in the yield or purity of the desired product, $[Ru^{VI}(TPP)(O)_2]$.

The aim of this work was to provide a reproducible synthesis of $[Ru^{VI}(TPP)(O)_2]$, and to achieve a deeper understanding of its structure and reactivity. Key to the success of this goal was the use X-ray powder diffraction (XRPD) methods, both to solve ab initio the structure of complexes for which single crystals could not be grown and to assess the purity of the same compounds. XRPD, as a highly accurate structural and analytical tool, was indeed employed in the characterization of, among others, the $[Ru^{VI}(TPP)(O)_2]$ species, which, as later discussed, exhibits nontrivial behavior in solution and is unstable in many solvents. The numbering scheme for the relevant ruthenium tetraphenylporphyrinate derivatives is given in Chart 1.

(15) Ho, C.; Leung, W.-H.; Che, C.-M. *J. Chem. Soc., Dalton Trans.* **1991**, 2933−2939.
(16) Masuda, H.; Taga, T.; Osaki, K.; Sugimoto, H.; Mori, M.; Ogoshi, H. *J. Am. Chem. Soc.* **1981**, *103*, 2199−2203.
(17) Mosseri, S.; Neta, P.; Hambright, P. *J. Phys. Chem.* **1989**, *93*, 2358−2362 and reference therein.
(18) Che, C.-M.; Yu, W.-Y. *Pure Appl. Chem.* **1999**, *71*, 281−288.

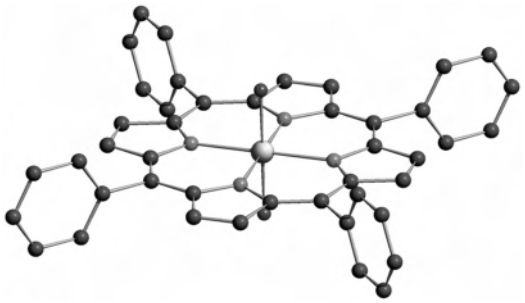

Figure 1. Schematic drawing of the molecular structure of the $[Ru^{VI}(TPP)(O)_2]$ species (**3**) showing the two oxo fragments trans to each other. Selected distances for **3**: 2.14(6) Å for the Ru−N distance and 1.74(1) Å for the Ru−O distance.

Results and Discussion

Synthesis of $[Ru^{VI}(TPP)(O)_2]$ (3) and $[Ru^{IV}(TPP)(OH)]_2$-(O) (4). Che and co-workers reported that **3** can be obtained by oxidation of [Ru(TPP)(CO)(MeOH)] (**2**) by *m*-CPBA in EtOH[11a] or in a $EtOH/CH_2Cl_2$[15,18] mixture as solvents, but in the latter case, some quantitative details of the experimental procedures (such as solvent amounts) have never been published. We have performed an extensive investigation of the effect of the solvent composition and the oxidant amount. Under the best experimental conditions (5:1 $EtOH/CH_2Cl_2$ mixture and 20:1 *m*-CPBA/**2**), complex **3** was formed selectively and was isolated in a 78% yield by simple filtration of the resulting suspension without the need for any further purification. Single crystals of **3** could not be grown, at least in part because it decomposes on long standing in most solvents which dissolve it. However, the structure of this complex could be determined by ab initio XRPD on the crude (polycrystalline) solid (Figure 1).

The perfect coincidence between the experimental and simulated XRPD patterns also allows to state that the material obtained under the best experimental conditions has a very high purity, no amorphous halo, and no extra peaks being observed (see the Experimental Section).

The outcome of some of the other reactions performed in this optimization study is worth mentioning.

(a) If ethanol alone is employed as solvent, a viscous suspension of a very fine material is obtained, from which the product could not be efficiently separated by either filtration or centrifugation. Addition of CH_2Cl_2 to this mixture after the reaction was completed improved filterability, but the product was found to contain only a small amount of **3**, accompanied by several byproducts.

(b) If CH_2Cl_2 alone is employed as a solvent, the product is not **3**, but the μ-oxo dimeric complex, $[Ru^{IV}(TPP)(OH)]_2$-(O) (**4**). The complex was isolated, as a pure polycrystalline phase, in ∼60% yield and was, again, structurally characterized by ab initio XRPD (Figure 2). Several complexes of the general [Ru(porphyrin)OR]$_2$O type (R = H, alkyl, or aryl) have been described in the literature, and the X-ray structures of two of them have been reported.[14a,16] However, despite the fact that **4** has been said to be a byproduct in the synthesis of **3**, it has never been isolated in a pure form, nor was it fully characterized before.

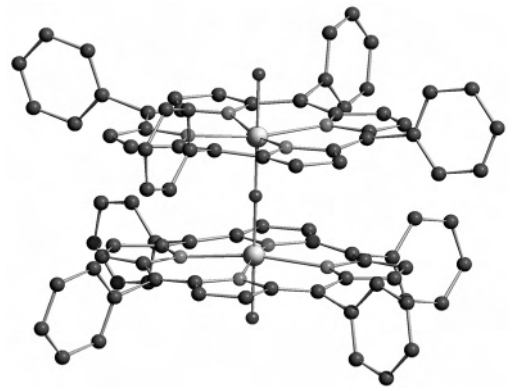

Figure 2. Schematic drawing of the molecular structure of the $[Ru^{IV}(TPP)(OH)]_2O$ species (**4**) showing the two hydroxo and the μ-oxo fragments trans to each other. Selected distances for **4**: 2.13(1) Å for the Ru−N distance, 1.90(6) Å for the Ru−O distance, and 2.11(3) Å for the Ru−OH distance.

(c) Provided the correct solvent mixture is employed, **3** could equally well be synthesized starting from [Ru(TPP)(CO)] (**1**) instead of its methanol adduct [Ru(TPP)(CO)(CH_3OH)] (**2**). Together with the result of the experiment described just above, this implies that the presence of a sixth ligand in the starting complex is not influential and that the solvent composition is the important parameter in driving the reaction toward the formation of **3** or **4**.

(d) If THF is employed in a mixture with CH_2Cl_2 in place of ethanol under the optimized conditions, **3** is still the major product, but a large amount of **4** is also formed.

(e) In general, a large excess of oxidant is required to consume all of the starting **1** or **2**. The minimum *m*-CPBA:Ru molar ratio also depends on the solvent composition and is 15 in neat ethanol, but is reduced to ~10 in a 1:10 CH_2Cl_2/EtOH mixture. In neat CH_2Cl_2, a 7:1 molar excess of *m*-CPBA with respect to ruthenium is sufficient to consume all of the starting complex, but as previously mentioned, the only isolated product was **4**. In CH_2Cl_2, **4** remained the only product even if a larger excess (20:1) of *m*-CPBA was employed, indicating that the outcome of the reaction is not dictated by a low concentration of the acid in solution. Under our experimental conditions (*m*-CPBA as the oxidizing agent), **4** could not be further oxidized to **3**.

(f) When nonideal solvents or oxidant amounts were employed, the isolated solid contained a mixture of **3** and **4**. It should be recalled that $[Ru(TPP)(OR)]_2O$ complexes (R = Me or Et) have been reported in the literature and found to exchange the terminal alkoxy group with another alcohol or with water very easily in the presence of acids.[14a] The crystallographically characterized species **4** never contacted any alcohol, so no doubt can be raised about its identity. On the other hand, we cannot exclude the possibility that the compound identified by ^{1}H NMR as **4** in mixtures obtained from EtOH and CH_2Cl_2 is at least in part the ethoxy $[Ru(TPP)(OEt)]_2O$ derivative. However, we never detected in the ^{1}H NMR spectrum of these mixtures run in $CDCl_3$ the signals at −3.86 and −4.03 ppm, which are diagnostic of the ethoxy group in the axial position of the porphyrin complex.[14a] Since the solvents employed for the synthesis of **4** have never been dried, it appears that the equilibrium is shifted on the side of the hydroxo complex even in the presence of an excess of ethanol.

Scheme 2. Alternative Pathways Leading to the Formation of $[Ru^{IV}(TPP)(OH)]_2O$ (**4**)

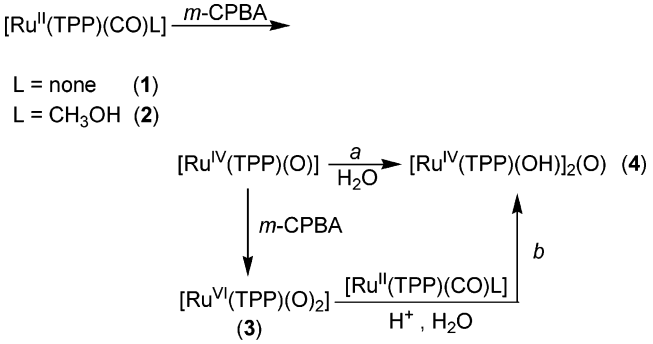

Moreover, to better understand the reaction mechanism, we also investigated the reaction of **2** with **3**. When equimolar amounts of **2** and **3** are dissolved in CH_2Cl_2 at room temperature, no reaction occurs, at least for several hours. However, if a small amount of hydrochloric or *m*-chlorobenzoic acid is added, a reaction yielding the μ-oxo dimer **4** is observed (path b in Scheme 2). The promotional effect of acids on the reactivity of related porphyrin complexes has previously been noted,[13b−d,i] but to the best of our knowledge, the coproportionation reaction of **2** and **3** to give **4** has never been reported.

The aforementioned data, taken together, allow us to shed some light on the mechanism of the formation of **3** and **4** by reaction of **1** or **2** with *m*-CPBA. In the literature, the reaction has been proposed to start with the oxidation of **1** or **2** to a mono-oxo-Ru^{IV} intermediate. In the absence of coordinating ligands, this complex dimerizes to afford **4** (path a in Scheme 2), also in agreement with the mechanism proposed for the reaction of **1** with dioxygen (Scheme 1). However, THF is a coordinating solvent as ethanol, yet it only partly inhibits the formation of **4**. Therefore, there must be a second role for ethanol which explains why in its presence the reaction can become completely selective. During the synthesis, acids (*m*-CPBA and its deoxygenated analogue *m*-chlorobenzoic acid) are present in large amounts, and our results imply that the formed **3** should immediately react with the remaining **1** or **2** if either is present in solution (path b in Scheme 2). The second role of ethanol is now easily identified when we consider that **1** and **2** are poorly soluble in this solvent and, worth noting, **3** is virtually insoluble in it. Thus, ethanol acts as a precipitating solvent for the product and prevents it from reacting with the remaining starting material. THF, which is not a precipitating agent for **3**, is, therefore, less effective in preventing the formation of **4**.

Solution Behavior and ^{1}H NMR Spectra of $[Ru(TPP)(O)_2]$ (3). When a high-purity (XRPD evidence) sample of **3** was dissolved in $CDCl_3$, two sets of signals were observed. The first set of signals, marked with an asterisk in Figure 3, can be attributed to the highly symmetric monomeric $[Ru^{VI}(TPP)(O)_2]$ (**3a**). The D_{4h} symmetry is retained in solution, and one signal was observed at 9.10 ppm corresponding to eight pyrrolic hydrogen atoms (H_β) along with two signals in the aromatic region, one for the eight *ortho* hydrogen

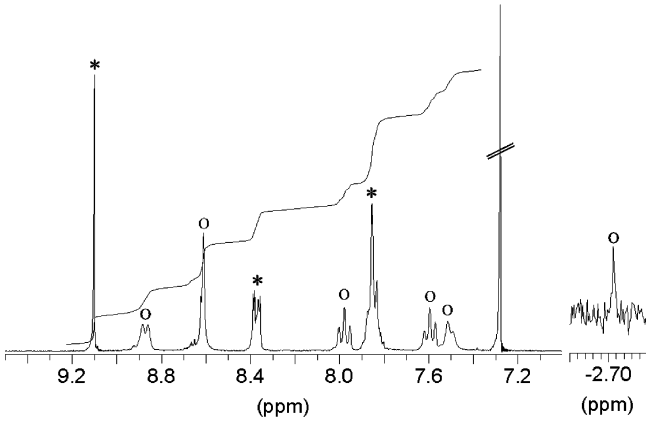

Figure 3. ^{1}H NMR spectrum of **3** in $CDCl_3$.

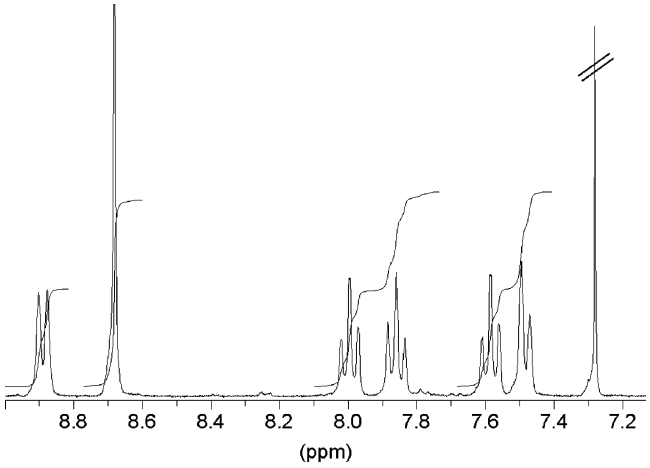

Figure 4. ^{1}H NMR spectrum of **4** in $CDCl_3$.

atoms (8.38 ppm) and one for the eight *meta* hydrogen atoms which overlap with the four *para* hydrogen atoms (7.85 ppm).[19]

The second pattern observed, marked with an empty circle in Figure 3, belongs to a species with apparently lower symmetry (**3b**) in which the signals for the eight *ortho* hydrogen atoms and for the eight *meta* hydrogen atoms split into two sets of signals each and the pyrrolic protons resonate at higher fields (8.61 ppm). This pattern indicates that the plane of symmetry determined by the porphyrin ring is lost, as usually happens for dimeric porphyrin complexes. The species producing this last set of signals is always present in any spectrum of **3** we recorded in this solvent. It should not be confused with **4**, whose spectrum in the same solvent is reported in Figure 4. For the latter, the pyrrolic protons resonate at 8.67 ppm and can indeed be observed when samples obtained under nonoptimized conditions are analyzed. In the ^{1}H NMR spectrum of **3**, a singlet was also present at −2.70 ppm, indicating that the hydrogen atoms that produce it are in the shielding cone of the porphyrin. The same situation was observed when CD_2Cl_2 or C_6D_6 was employed in place of $CDCl_3$, although in C_6D_6 a poorly defined spectrum was obtained, due to the low solubility of **3** in this solvent.

(19) The spectrum described here correlates well with the one reported by Che and co-workers in Figure 3 in ref 11a for the same product. However, the latter does not correspond exactly to the one described in the Experimental Section of the same paper.

The relative intensity of the signals in our spectra in solution would imply that the **3a**:**3b** ratio ≅ 3:1, which is inconsistent with the data obtained in the solid state by XRPD, which indicate that only one species is present. The second group of signals did not disappear when the solution was filtered through Celite, indicating that it is not due to incompletely dissolved material. The relative ratio of the two species remained almost unchanged even using strictly anhydrous $CDCl_3$ (freshly distilled over CaH_2) or if H_2O or D_2O was added to the solution, at least on the minute time scale. Investigations over long period of times of solutions of **3** are hampered by the formation of variable amounts of **4** upon prolonged standing, especially when water had been added. Of note is the fact that the signal at −2.70 ppm did not disappear after addition of D_2O. Moreover, samples of **3** always contained some water, even if heated in vacuo for several hours. The only observable phenomenon, when samples containing smaller amounts of water are examined, is a shift to higher fields (from 1.55 to 0.5 ppm) in the position of the water signal itself. In the case of **3**, two cavities (per unit cell) with a volume of ∼45 Å^3 each, i.e., comparable with that of water molecules, are present. The shortest O···H distance would lie at ∼2.8 Å; thus, we cannot exclude the partial occupancy of these cavities by occluded water molecules, not visible by XRPD. To exclude the possibility that **3** reacts with $CDCl_3$, a solution of the product for which an ^{1}H NMR spectrum had been recorded was evaporated in a vacuum and analyzed by XRPD. Its diffraction pattern was found to be that of the starting [Ru(TPP)(O)$_2$] species, **3**. Identical results were obtained when **3** was treated in C_6H_6.

To investigate the nature of the second species, we performed PGSE (pulsed field gradient spin-echo) NMR measurements[20] on $CDCl_3$ solutions of **3** using the standard stimulated echo pulse sequence at room temperature. These measurements can afford specific information about the size of the species present in solution, in that the hydrodynamic radii and the volumes of the diffusing particles can be estimated.[21] According to the Stokes−Einstein equation (eq 1), the diffusion coefficient (D_t) is inversely proportional to the hydrodynamic radius (r_H) of the diffusing particle.

$$D_t = \frac{kT}{6\pi\eta r_H} \qquad (1)$$

where k is the Boltzmann constant, T is the absolute temperature, and η is the viscosity of the medium. Consequently, the volume (V) of the diffusing particle that in the Stokes−Einstein model is assumed to be spherical is inversely proportional to D_t^3.

(20) Johnson, C. S., Jr. *Prog. Nucl. Magn. Reson. Spectrosc.* **1999**, *34*, 203−256 and references therein.

(21) For some recent references, see: (a) Babushkin, D. E.; Brintzinger, H.-H. *J. Am. Chem. Soc.* **2002**, *124*, 12869−12873. (b) Burini, A.; Fackler, J. P., Jr.; Galassi, R.; Macchioni, A.; Omary, M. A.; Rawashdeh-Omary, M. A.; Pietroni, B. R.; Sabatini, S.; Zuccaccia, C. *J. Am. Chem. Soc.* **2002**, *124*, 4570−4571. (c) Drago, D.; Pregosin, P. S.; Pfaltz, A. *Chem. Commun.* **2002**, 286−287. (d) Macchioni, A.; Romeni, A.; Zuccaccia, C.; Guglielmetti, G.; Querci, C. *Organometallics* **2003**, *22*, 1526−1533. (e) Pregosin, P. S.; Martínez-Viviente, E.; Kumar, P. G. A. *Dalton Trans.* **2003**, 4007−4014.

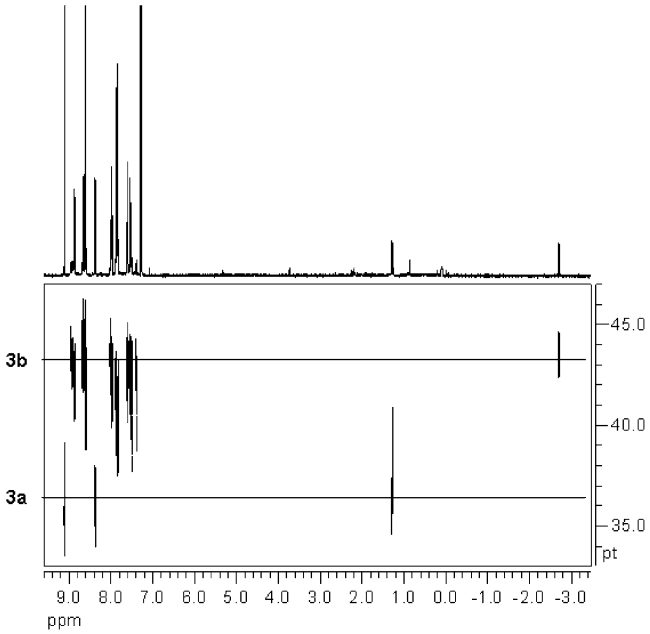

Figure 5. DOSY display of **3** at 500 MHz.

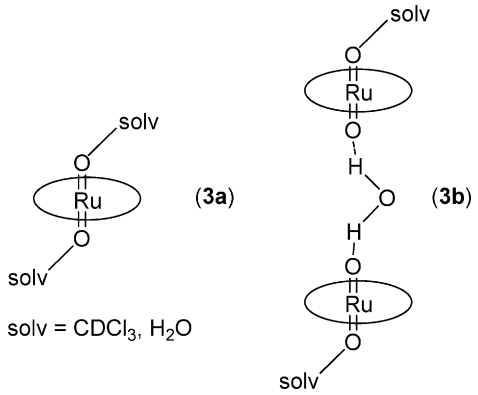

Figure 6. Proposed solution structures for **3a** and **3b**.

The V_{3b}:V_{3a} ratio was calculated as $(D_{3a}/D_{3b})^3$, obtaining a volume ratio of 2.0:1, indicating that **3b** is a dimer with respect to **3a**. Noteworthy, the signal at −2.70 ppm also belongs to the dimer and must be associated with it (Figure 5).

Both **3a** and **3b** undergo extremely fast reactions in the presence of a suitable reductant. This has been shown by adding a 4-fold excess of Ph_3P to a solution of **3** in $CDCl_3$.[11d] An instantaneous reaction occurred; no intermediate could be detected at room temperature, and the only observed complex was $[Ru^{II}(TPP)(PPh_3)_2]$.[22] The ^{31}P NMR spectrum of the reaction mixture showed the presence of Ph_3PO also.

In conclusion, even if an unequivocal characterization of the second species cannot be given, all available experimental evidence points to **3a** and **3b** being two different solvates of **3**. In particular, **3b** appears to be a dimeric species held together by hydrogen bonding to a water molecule (Figure 6). Note that at this stage we cannot exclude the presence of two bridging water molecules.

(22) Ariel, S.; Dolphin, D.; Domazetis, G.; James, B. R.; Leung, T. W.; Rettig, S. J.; Trotter, J.; Williams, G. M. *Can. J. Chem.* **1984**, *62*, 755−762.

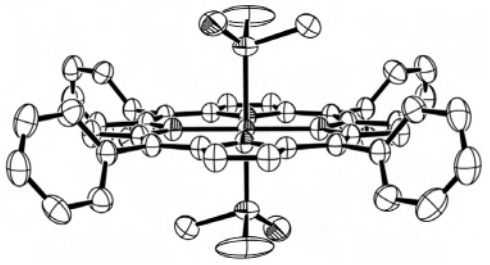

Figure 7. ORTEP drawing of the molecular structure of the $[Ru^{II}(TPP)(S\text{-}DMSO)_2]$ species (**5**) showing the two DMSO molecules trans to each other. Only one conformation of the disordered phenyl fragments and DMSO molecules has been reported for clarity. Selected distances for **5**: 2.043(2)−2.046(2) Å for the Ru−N distance and 2.3140(7) Å for the Ru−S distance.

The position of the bridging molecule explains both why it does not exchange with external D_2O and why it resonates at negative fields in the ^1H NMR spectra. The stability of **3b** suggests that even the Ru═O groups not involved in dimer formation should form strong hydrogen bonds. This is in full agreement with the observed shift in the position of the water signal. This can now be easily explained by a time-mediated exchange of free water molecules with the ones hydrogen bonded to the "terminal" Ru═O groups. Clearly, even chloroform itself can form a hydrogen bond to the Ru═O group, but because it is present in a large excess, no shift is detectable.

Reaction of $[Ru(TPP)(O)_2]$ with Dimethyl Sulfoxide and Synthesis of $[Ru(TPP)(S\text{-}DMSO)_2]$ (5). When a sample of **3** was dispersed in $(CD_3)_2SO$, a heterogeneous mixture was obtained, which showed in the ^1H NMR spectrum many ill-resolved signals (as expected for a dispersion of small particles). When the temperature was increased to 110 °C, the solid material completely dissolved and the complex pattern disappeared, leading to a much simpler ^1H NMR spectrum (see the Experimental Section). This spectrum belongs to a species with apparent D_{4h} symmetry, and shows a singlet at 8.42 ppm (assigned to eight pyrrolic protons) and multiplets centered at 8.08 and 7.76 ppm, for the eight *ortho* and twelve *meta* and *para* aromatic protons, respectively. Interestingly, this pattern was conserved when the sample was cooled to room temperature. Despite the similarity of the spectra of **3** and **5**, the two species turned out to be different. Indeed, when this dissolution process was repeated on a preparative scale and the product isolated by precipitation and redissolved in $CDCl_3$, a spectrum different from the one of **3**, but still showing D_{4h} symmetry, was observed.

The new species was unequivocally characterized as $[Ru(TPP)(S\text{-}DMSO)_2]$ (**5**) by conventional single-crystal X-ray diffraction analysis (Figure 7).

The synthesis of **5** has already been reported in the literature.[23] $[Ru(TPP)(S\text{-}DMSO)_2]$ was prepared by photolyzing [Ru(TPP)(CO)(ROH)] in DMSO solution. Other $[Ru(porphyrin)(S\text{-}DMSO)_2]$ complexes have been obtained using the same procedure described above[24] or by reacting the $[Ru(porphyrin)]_2$ dimer, which has been prepared by photolysis,

(23) Levine, L. M. A.; Holten, D. *J. Phys. Chem.* **1988**, *92*, 714−720.

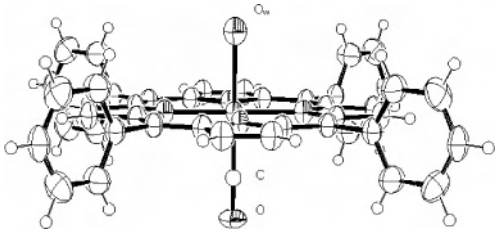

Figure 8. ORTEP drawing of the molecular structure of the [Ru^{II}(TPP)(CO)(H_2O)] species (**6**) showing the carbonyl (CO) and the water molecule (O_w) trans to each other. Water hydrogen atoms are not shown. Selected distances for **6**: 1.75(7) Å for the Ru−C distance, 2.045(3) Å for the Ru−N distance, and 2.22(4) Å for the Ru−O distance.

in the presence of DMSO.[25] Our synthesis does not require any specialized equipment, such as medium-pressure mercury lamps or lasers, at any stage of the reaction and appears to be more suited for the preparation of large amounts of **5**, which can be regarded as an interesting starting material for the synthesis of other ruthenium−porphyrin complexes. It should also be noted that related [Ru(porphyrin)L_2] complexes (L = arylamine or alkylamine) have been obtained by reaction of [Ru(porphyrin)$(O)_2$] with amines or hydroxylamines.[11c,26]

Reduction of [Ru(TPP)(O_2)] (3) by Carbon Monoxide. During recent work in our laboratories on the reactivity of aryl azides with **1** and **2**, we isolated a [Ru^{IV}(TPP)(CO)(ArN)] complex having an imido group coordinated to a ruthenium(IV) center.[27] With this result in mind, we decided to test if an analogous complex could be isolated having an oxo ligand in place of the imido one. Toward this aim, we subjected **3** to a CO atmosphere in CH_2Cl_2. No reaction was observed at atmospheric CO pressure, but when the reaction was conducted under 60 bar of CO in an autoclave, a crystalline product, **6**, precipitated out of the solution. Some of the crystals were of sufficient quality for determining the single-crystal X-ray structure (Figure 8). The remaining polycrystalline material was analyzed by XRPD and found to be identical with the single crystal. Thus, the *whole* obtained material is composed by the same complex, and the single crystals are highly representative of the bulk composition.

The obtained complex (Figure 8) has a coordinated CO ligand, and the opposite position in the coordination sphere is occupied by an oxygen atom. However, the refined Ru−O distance (2.24 Å) is inconsistent with the formulation of this group as an oxo ligand (the expected Ru=O distance lies in the 1.66−1.82 Å range) and indicates a single-bond character for this interaction. The isolated complex may thus be [Ru^{III}(TPP)(CO)(OH)] (**A**) or [Ru^{II}(TPP)(CO)(H_2O)] (**B**). Aquo

Scheme 3. Reaction of [Ru(TPP)$(O)_2$] (**3**) with Carbon Monoxide

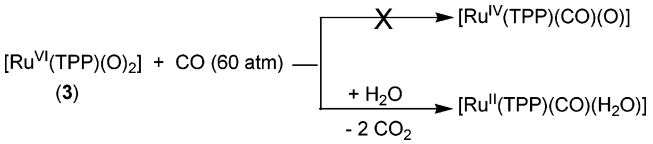

complexes with the [Ru(porphyrin)(CO)(H_2O)] general formula have been isolated as single crystals in a few cases,[9a,13f,28] but apparently, no bulk material having this composition has ever been obtained. It has been suggested that the water molecule in these complexes is very labile and that its coordination must be stabilized by hydrogen bonding.

The UV−visible spectrum of **6** is indistinguishable from those of **1** and **2**. Moreover, the compound is diamagnetic at room temperature, and no EPR signal was observed to 100 K. All these data indicate that complex **6** has formulation **B** above (Scheme 3).

This assignment was further confirmed by an independent synthesis of **6** from **2** in a boiling ethyl acetate/water mixture (see the Experimental Section). Finally, reaction of **6** with *tert*-butylpyridine afforded the previously reported [Ru(TPP)(CO)(4-^{t}Bu-Py)].[29] The water included in **6** during its preparation from **3** must originate from the CO gas, of which it represents the main contaminant.

Characterization of "[Ru(TPP)(CO)]". The [Ru(TPP)(CO)] complex (**1**) is the entry point for most ruthenium−tetraphenylporphyrin chemistry and is even commercially available, but has been characterized less thoroughly than may be expected. It is generally synthesized by reaction of $TPPH_2$ with $Ru_3(CO)_{12}$ in refluxing Decaline or toluene, and the product is purified by column chromatography on silica. However, different preparations of **1** with the synthetic method described above afford materials that show slightly different ν_{CO} stretching frequencies (in our hands, in the range of 1950−1956 cm^{-1}) even when measured on the same instrument. By comparison, both [Ru(TPP)(CO)(H_2O)] (**6**) and [Ru(TPP)(CO)(MeOH)] (**2**) reproducibly exhibit an IR absorption at 1949 cm^{-1}.

We originally attributed the variability of the observed CO stretching frequency in the solid to the presence of different crystal packing forms (i.e., polymorphs), but XRPD measurements on several samples allowed us to discard this possibility. Indeed, the [Ru(TPP)(CO)] complex crystallizes in only one form, a tetragonal phase isomorphous with **6** and **2**. This should not be a surprise, since the crystal packing is mostly dictated by the mutual interlocking of the phenyl rings of the TPP moieties. However, we found that a small, but non-negligible, variability existed in the refined lattice parameters of [Ru(TPP)(CO)] from different preparations (although fully maintaining the *I*4/*m* crystal symmetry). In addition, a slight improvement of the agreement factors of

(24) (a) Hopf, F. R.; O'Brien, T. P.; Scheidt, W. R.; Whitten, D. G. *J. Am. Chem. Soc.* **1975**, *97*, 277−281. (b) Ikonen, M.; Guez, D.; Marvaud, V.; Markovitsi, D. *Chem. Phys. Lett.* **1994**, *231*, 93−97.
(25) (a) Pacheco, A.; James, B. R.; Rettig, S. J. *Inorg. Chem.* **1995**, *34*, 3477−3484. (b) Pacheco, A.; James, B. R.; Rettig, S. J. *Inorg. Chem.* **1999**, *38*, 5579−5587.
(26) (a) Huang, J.-S.; Sun, X.-R.; Leung, S. K.-Y.; Cheung, K.-K.; Che, C.-M. *Chem.−Eur. J.* **2000**, *6*, 334−344. (b) Liang, J.-L.; Huang, J.-S.; Zhou, Z.-Y.; Cheung, K.-K.; Che, C.-M. *Chem.−Eur. J.* **2001**, *7*, 2306−2317. (c) Leung, S. K.-Y.; Huang, J.-S.; Liang, J.-L.; Che, C.-M.; Zhou, Z.-Y. *Angew. Chem., Int. Ed.* **2003**, *42*, 340−343.
(27) S. Cenini et al., unpublished results.
(28) (a) Kadish, K. M.; Hu, Y.; Mu, X. H. *J. Heterocycl. Chem.* **1991**, *28*, 1821−1824. (b) Slebodnick, C.; Kim, K.; Ibers, J. A. *Inorg. Chem.* **1993**, *32*, 5338−5342. (c) Birnbaum, R. A.; Schaefer, W. P.; Labinger, J. A.; Bercaw, J. E.; Gray, H. B. *Inorg. Chem.* **1995**, *34*, 1751−1755.
(29) Eaton, S. S.; Eaton, G. R.; Holm, R. H. *J. Organomet. Chem.* **1972**, *39*, 179−195.

the pertinent structural refinements could be achieved by partially occupying the "empty" coordination site with a water molecule. The following observations finally solve the problem.

(a) The IR spectrum of the crude material before the chromatographic separation exhibits an absorption at 1956 cm^{-1}, although other bands can also be attributed to $Ru_3(CO)_{12}$ used as a starting material.

(b) In one experiment, a sample of [Ru(TPP)(CO)] was obtained by precipitating the compound at room temperature from a chloroform/ethyl acetate fraction of the chromatographic column. The sample was briefly dried in a dinitrogen stream without either heating it or placing it in vacuo. The IR spectrum of the material so obtained exhibited a ν_{CO} of 1950 cm^{-1}.

(c) If the sample of [Ru(TPP)(CO)] precipitated from the solution is heated in vacuo at 120 °C, the ν_{CO} stretching gradually moves from 1950 to 1956 cm^{-1} over a few hours.

(d) The thermogravimetric curves of different [Ru(TPP)(CO)] samples exhibited rather erratic behavior, with weight losses, at 250 °C, of 3−5%.

All this experimental evidence leads us to the following conclusions.

(1) The compound usually formulated as [Ru(TPP)(CO)] is actually a solid-state solution in which variable proportions of pristine [Ru(TPP)(CO)] and [Ru(TPP)(CO)(H_2O)] can be present. The ν_{CO} absorptions of the two complexes are too close to be separated even when working at a 1 cm^{-1} resolution. Therefore, only one band is observed, the position of which depends on the relative proportion of the two complexes in the mixture.

(2) In the synthesis, authentic [Ru(TPP)(CO)] is initially formed, which is quantitatively transformed in [Ru(TPP)(CO)(H_2O)] during the chromatographic purification, water clearly originating from silica itself or from moist solvents.

(3) When the solutions obtained by the chromatographic purification are evaporated and the resulting solid is heated in vacuo to remove the last traces of solvent, part of the coordinated water is released (in a poorly reproducible way), causing the observed variation of the IR spectrum.

(4) The shifts of the peak positions of the measured XRPD patterns (well above the instrumental reproducibility) are, thus, a manifestation of the different compositions of the differently prepared samples (see Figure 9).

(5) Accordingly, the TG traces, showing different slopes in the 100−400 °C range, speak for (at least) three nearly overlapping events {i.e., water and CO elimination, as well as sublimation of the "$[Ru(TPP)]_n$" species}; indeed, dissociation of 1 mol of CO or H_2O implies a 3.8 or 2.4% weight loss, respectively.

Experimental Section

Unless otherwise specified, all reactions and manipulations were performed in air using magnetic stirring. The solvents for the syntheses were of analytical grade, except for Decalin (sodium) which was dried, distilled, and stored under dinitrogen. *m*-Chloroperoxybenzoic acid (77%, Aldrich) and triphenylphosphine (99%, Aldrich) were used as received. Ruthenium dodecacarbonyl,[30] tetraphenylporhyrin,[31] [Ru(TPP)(4-^{t}Bu-Py)(CO)],[29] and [Ru(TPP)(CH_3OH)(CO)] (**2**)[32] were prepared according to literature procedures. ^{1}H NMR and ^{31}P NMR spectra were recorded on Advanced 300-DRX Bruker instruments. PGSE measurements were performed on an Advanced 500-DRX Bruker spectrometer equipped with a QNP probe with a Z-gradient coil. Infrared spectra were obtained as Nujol mulls on a Bio-Rad FTS-7 spectrophotometer. UV−visible spectra were recorded on a Hewlett-Packard 8452A spectrophotometer. Thermogravimetric experiments were performed on a Perkin-Elmer TGA 7 instrument. Elemental analyses and mass spectra were recorded in the analytical laboratories of Milan University.

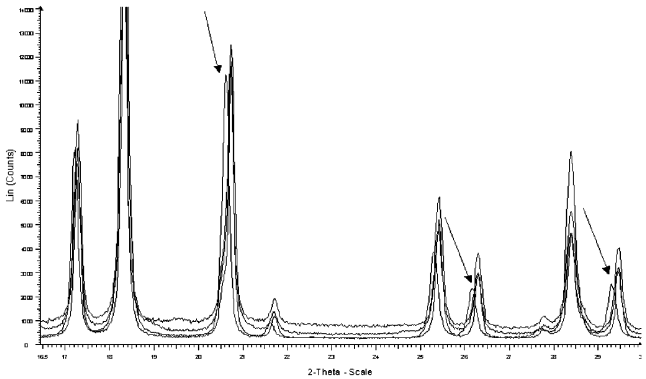

Figure 9. Selected portion ($16.5° < 2\theta < 30°$) of different XRPD patterns of species of nominal [Ru(TPP)(CO)] formula (from four different preparations), showing the small, though significant, variability of the peak positions (see arrows). Whole-profile (structureless) refinements by the Le Bail method and corrections for sample displacement errors allowed us to assess the variability of the lattice parameters, which ranged from 13.538 to 13.613 Å and from 9.683 to 9.688 Å for *a* and *c*, respectively (the length of the tetragonal axis being nearly constant), in agreement with a solid solution behavior.

Preparation of [Ru(TPP)(CO)] (1). A modification of the procedure of Rillema et al.[32] was used. $Ru_3(CO)_{12}$ (0.575 g, 0.899 mmol) and $TPPH_2$ (1.24 g, 2.03 mmol) were suspended in dry Decalin (50 mL) under a dinitrogen atmosphere. The reaction mixture was refluxed for 4 h, and the resulting solid was collected in a filter and washed with *n*-hexane (3 × 10 mL) to remove Decalin. The violet solid was then purified by flash chromatography on silica. Toluene was used to elute unreacted $Ru_3(CO)_{12}$, a 7:3 CH_2Cl_2/*n*-hexane mixture to elute $TPPH_2$, and finally $CHCl_3$ to yield **1** (1.03 g, 69%): ^{1}H NMR (300 MHz, $CDCl_3$, 300 K) δ 8.71 (s, 8H, H_β), 8.26 (m, 4H, H_o), 8.15 (m, 4H, H_o), 7.75 (m, 12H, H_{m-p}); IR (Nujol) $\nu = 1950-1956$ cm^{-1} (CO, see Characterization of [Ru(TPP)(CO)] in the Results and Discussion), 1008 cm^{-1} (oxidation marker); UV−vis (CH_2Cl_2) λ_{max} (log ϵ_M) = 588 (3.51), 528 (4.29), 412 nm (5.38). Anal. Calcd for $C_{45}H_{28}N_4ORu$ (741.81): C, 72.86%; H, 3.80%; N, 7.55%. Found: C, 72.38%; H, 4.05%; N, 7.22%.

Preparation of [Ru(TPP)(O)$_2$] (3). A modification of the procedure of Che[15] was used. In the optimized procedure, *m*-CPBA (1.67 g, 7.43 mmol) was dissolved in EtOH (40 mL) and the resulting solution was added in one portion to an orange suspension of **2** (0.298 g, 0.385 mmol) in CH_2Cl_2 (10 mL) and EtOH (10 mL). The resulting dark suspension was stirred for 1 h, and the dark

(30) Eady, C. R.; Jackson, P. F.; Johnson, B. F. G.; Lewis, J.; Malatesta, M. C.; McPartlin, M.; Nelson, W. J. H. *J. Chem. Soc., Dalton Trans.* **1980**, 383−392.
(31) Adler, A. D.; Longo, F. R.; Finarelli, J. D.; Goldmacher, J.; Assour, J.; Korsakoff, L. *J. Org. Chem.* **1967**, *32*, 476.
(32) Rillema, D. P.; Nagle, J. K.; Barringer, L. F., Jr.; Meyer, T. J. *J. Am. Chem. Soc.* **1981**, *103*, 56−62.

Table 1 [a]

Synoptic Collection of Crystal Data for the Four Structurally Characterized Species

	[Ru(TPP)(O)$_2$] (**3**)	[Ru(TPP)(OH)]$_2$(O) (**4**)	[Ru(TPP)(*S*-DMSO)$_2$] (**5**)	[Ru(TPP)(CO)(H$_2$O)] (**6**)
formula	$C_{44}H_{28}N_4O_2Ru$	$C_{88}H_{56}N_8O_3Ru_2$	$C_{48}H_{40}N_4O_2RuS_2$	$C_{45}H_{30}N_4O_2Ru$
fw (amu)	745.77	1477.56	870.03	759.80
cryst syst	tetragonal	tetragonal	monoclinic	tetragonal
space group	*I*4/*m*	*P*4/*nnc*	*I*2/*m*	*I*4/*m*
a (Å)	13.3992(4)	13.2334(4)	14.629(2)	13.558(2)
b (Å)	13.3992(4)	13.2334(4)	9.356(1)	13.558(2)
c (Å)	9.7116(3)	19.4274(7)	14.465(2)	9.685(1)
α (deg)	90	90	90	90
β (deg)	90	90	91.12(1)	90
γ (deg)	90	90	90	90
V (Å^3)	1743.6(1)	3402.2(2)	1979.4(2)	1780.2(2)
Z	2	2	2	2
D_{calc} (g/cm^3)	1.420	1.442	1.460	1.417
method	powder XRD	powder XRD	single-crystal XRD	single-crystal XRD

Details of Single-Crystal Analyses

	[Ru(TPP)(*S*-DMSO)$_2$]	[Ru(TPP)(CO)(H$_2$O)]
absorption coefficient (mm^{-1})	0.548	0.485
F(000)	896	776
cryst size	0.10 mm × 0.15 mm × 0.25 mm	0.15 mm × 0.15 mm × 0.30 mm
limiting indices	$-19 \le h \le 19$, $-12 \le k \le 12$, $-19 \le l \le 19$	$-16 \le h \le 16$, $-16 \le k \le 16$, $-11 \le l \le 11$
no. of reflections collected/unique	13697/2635 ($R_{int} = 0.029$)	9948/842 ($R_{int} = 0.080$)
absorption correction	Sadabs	Sadabs
refinement method	full-matrix least-squares on F^2	full-matrix least-squares on F^2
data/restraints/parameters	2635/0/205	842/0/76
goodness of fit on F^2	1.099	1.158
final *R* indices [$I > 2\sigma(I)$]	R1 = 0.036, wR2 = 0.094	R1 = 0.036, wR2 = 0.094

[a] $R_{int} = \sum|F_o^2 - F_o^2(\text{mean})|/\sum F_o^2$. $R_\sigma = \sum\sigma(F_o^2)/\sum F_o^2$. R1 = $\sum||F_o| - |F_c||/\sum|F_o|$. wR2 = $\{\sum[w(F_o^2 - F_c^2)^2]/\sum[w(F_o^2)^2]\}^{1/2}$. Goodness of fit = $[S/(n - p)]^{1/2} = \{\sum[w(F_o^2 - F_c^2)^2]/(n - p)\}^{1/2}$.

violet solid that formed was collected by filtration, washed with ethanol to remove the residual *m*-CPBA, and dried in a vacuum (0.22 g, 78%): ^{1}H NMR (300 MHz, $CDCl_3$, 300 K) monomeric species (**3a**) δ 9.10 (s, 8H, H_β), 8.38 (m, 8H, H_o), 7.85 (m, 12H, H_{m-p}), dimeric species (**3b**) δ 8.87 (m, 8H, H_o), 8.61 (s, 16H, H_β), 7.98 (m, 8H, H_m), 7.84 (m, 8H, H_p), 7.60 (m, 8H, H_m), 7.50 (m, 8H, H_o), −2.70 (s); ^{1}H NMR (300 MHz, CD_2Cl_2, 300 K) monomeric species δ 9.17 (s, 8H, H_β), 8.40 (m, 8H, H_o), 7.90 (m, 12H, H_{m-p}); dimeric species δ 8.92 (m, 8H, H_o), 8.66 (s, 16H, H_β), 8.02 (m, 8H, H_m), 7.90 (m, 8H, H_p), 7.62 (m, 8H, H_m), 7.48 (m, 8H, H_o), −2.80 (s); relative monomeric/dimeric species ratio ≅3/1; IR (Nujol) $\nu = 1017$ cm^{-1} (oxidation marker), 818 cm^{-1} (RuO_2); UV−vis (CH_2Cl_2) λ_{max} (log ϵ_M) = 542 (sh) (4.03), 520 (4.18), 418 nm (5.18). Anal. Calcd for $C_{44}H_{28}N_4O_2Ru$ (745.80): C, 70.86%; H, 3.78%; N, 7.51%. Found: C, 70.75%; H, 4.07%; N, 7.65%.

Preparation of [Ru(TPP)(OH)]$_2$O (4). In method a, a solution of *m*-CPBA (51.4 mg, 0.228 mmol) in CH_2Cl_2 (25 mL) was added to a suspension of **1** (104 mg, 0.14 mmol) in CH_2Cl_2 (35 mL). The resulting red solution was stirred overnight at room temperature and filtered through a short column of neutral alumina to yield **4** (62.2 mg, 61%). In method b, complex **3** (52.3 mg, 7.01×10^{-2} mmol) was added to a solution of **2** (53.8 mg, 6.95×10^{-2} mmol) in CH_2Cl_2 (60 mL) to yield a red solution that was stirred at room temperature for 30 min. After the addition of HCl (0.5 mL), the reaction mixture turned green and [Ru(TPP)(OH)]$_2$O was formed (TLC monitoring, CH_2Cl_2 as the eluant). The solution was then extracted with water (3 × 20 mL), and the organic layer was filtered through a short column of neutral alumina to yield **4** (56.9 mg, 55%). The same reaction was observed when using *m*-chlorobenzoic acid instead of hydrochloric acid: ^{1}H NMR (300 MHz, $CDCl_3$, 300 K) δ 8.89 (d, $J = 7.6$ Hz, 8H, H_o), 8.67 (s, 16H, H_β), 8.00 (t, $J = 7.6$ Hz, 8H, H_m), 7.86 (t, $J = 7.6$ Hz, 8H, H_p), 7.59 (t, $J = 7.6$ Hz, 8H, H_m,), 7.48 (d, $J = 7.6$ Hz, 8H, H_o); IR (Nujol) $\nu = 1014$ cm^{-1} (oxidation marker); UV−vis (CH_2Cl_2) λ_{max} (log ϵ_M) = 556 (4.30), 392 nm (5.58). Anal. Calcd for $C_{88}H_{58}N_8O_3Ru_2$ (1475.60): C, 71.63%; H, 3.83%; N, 7.59%. Found: C, 71.49%; H, 3.90%; N, 7.65%.

Preparation of [Ru(TPP)(*S*-DMSO)$_2$] (5). **3** (51.0 mg, 6.85×10^{-2} mmol) was suspended in DMSO (15 mL), and the resulting suspension was heated at 110 °C for 3 h. The total consumption of **3** was verified via TLC on alumina with dichloromethane as the eluent. The resulting pink solid was collected by filtration, washed with *n*-hexane, and dried in a vacuum (46.2 mg, 78%): ^{1}H NMR (300 MHz, $CDCl_3$, 300 K) δ 8.59 (s, 8H, H_β), 8.13 (m, 8H, H_o), 7.71 (m, 12H, H_{m-p}), −1.64 [s, 12H, $(CH_3)_2SO$]; ^{1}H NMR (300 MHz, DMSO-d_6, 300 K) δ 8.42 (s, 8H, H_β), 8.08 (m, 8H, H_o), 7.76 (m, 12H, H_{m-p}); IR (Nujol) $\nu = 1105$ cm^{-1} (S═O), 1006 cm^{-1} (oxidation marker); UV−vis (CH_2Cl_2) λ_{max} (log ϵ_M) = 524 (3.6), 414 nm (4.7). Anal. Calcd for $C_{48}H_{40}N_4O_2RuS_2$ (870.06): C, 66.26%; H, 4.63%; N, 6.44%. Found: C, 66.50%; H, 4.80%; N, 6.30%. Recrystallization from DMSO gave crystals suitable for X-ray analysis.

Preparation of [Ru(TPP)(CO)(H$_2$O)] (6). In method a, complex **1** (91.3 mg, 1.23 mmol) was suspended in a biphasic mixture of water (6 mL) and ethyl acetate (3 mL) and the resulting mixture was refluxed and vigorously stirred in air for 4 h. After the mixture had cooled, the aqueous layer was eliminated and the organic layer evaporated to dryness. The residue was boiled in *n*-hexane, and the resulting purple solid was then collected in a filter and dried in a vacuum (84.2 mg, 90%). In method b, a red solution of **3** (56.4

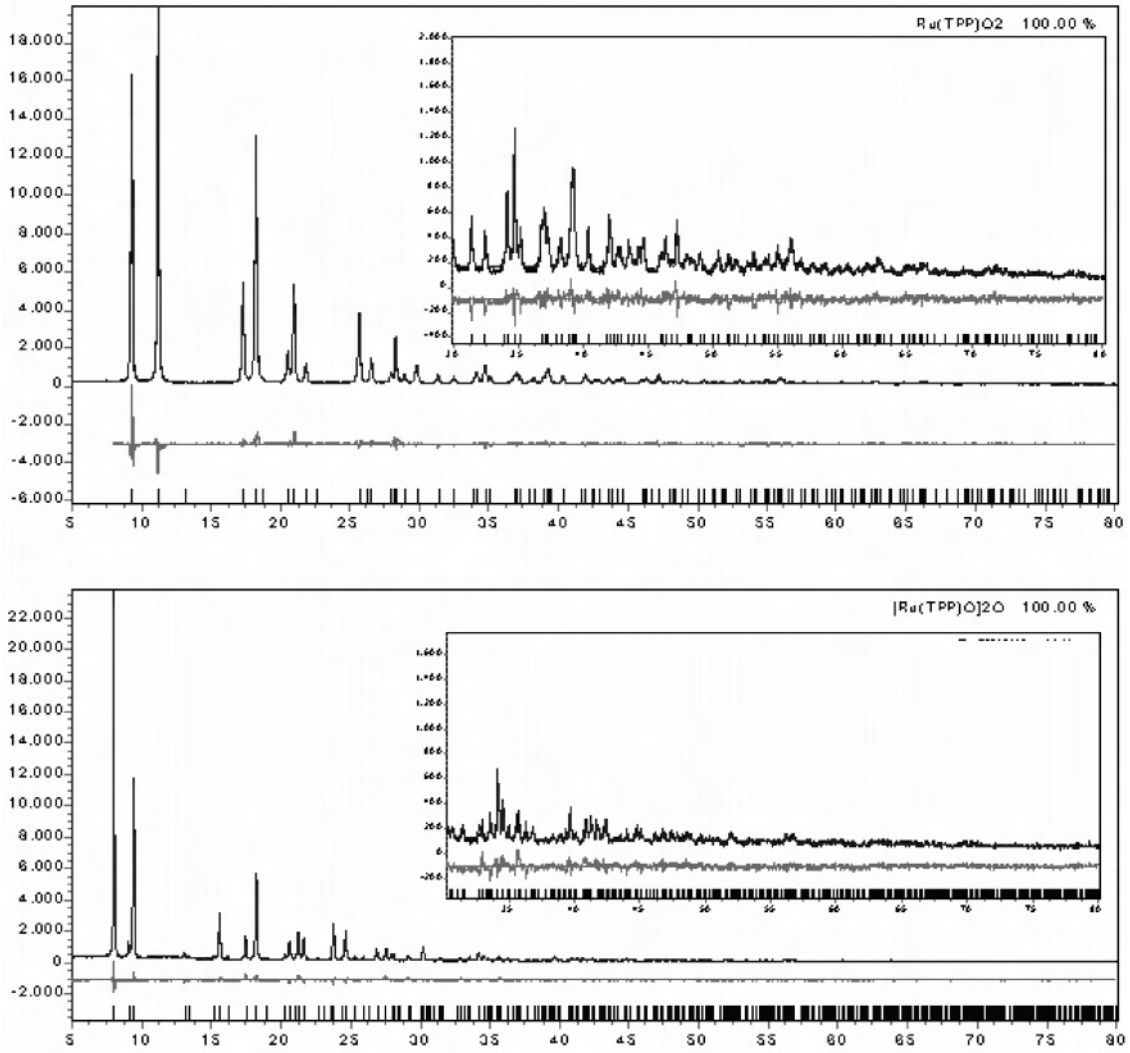

Figure 10. Rietveld refinement plots for $[Ru^{VI}(TPP)(O)_2]$ (**3**) (top) and $[Ru^{IV}(TPP)(OH)]_2O$ (**4**) (bottom). The horizontal axis is 2θ (degrees), and the vertical axis is counts. Difference plot and peak markers at the bottom. The sections above 30° (2θ) have been magnified in the insets.

mg, 7.56×10^{-2} mmol) in CH_2Cl_2 (15 mL) was placed in a glass liner inside an autoclave. The autoclave was frozen at dry ice temperature, evacuated, and filled with dinitrogen three times; then CO (60 bar) was added at room temperature, and the solution was stirred at room temperature for 5 h. The resulting purple solid was collected in a filter and dried in a vacuum (29.8 mg, 52%): ^{1}H NMR (300 MHz, $CDCl_3$, 300 K) δ 8.71 (s, 8H, H_β), 8.26 (m, 4H, H_o), 8.15 (m, 4H, H_o), 7.75 (m, 12H, H_{m-p}); IR (Nujol) $\nu = 1949$ cm^{-1} (CO), 1009 cm^{-1} (oxidation marker). Anal. Calcd for $C_{45}H_{30}N_4O_2Ru$ (759.83): C, 71.13%; H, 3.98%; N, 7.37%. Found: C, 70.85%; H, 4.12%; N, 7.05%. Recrystallization from CH_2Cl_2 gave crystals suitable for X-ray analysis.

Single-Crystal X-ray Analyses. Crystals of [Ru(TPP)(*S*-DMSO)$_2$] (**5**) and [Ru(TPP)(CO)(H_2O)] (**6**) suitable for X-ray crystallographic analysis were selected, attached to a glass fiber, and placed on the diffractometer. All data were collected at room temperature using a Bruker AXS diffractometer (equipped with Mo Kα radiation and a CCD area detector). Absorption corrections were applied using SADABS.[33] The WinGX suite of programs was used for the structure solutions and refinements.[34] The crystal structures were determined by direct methods and refined by full-matrix least-squares procedures. All non-hydrogen atoms were refined anisotropically. Split atom models were used to account for disorder of dimethyl sulfoxide and of the peripheral phenyls in **5** and of the CO/O_w in **6**. Hydrogen atoms were included in the refinement at calculated positions (apart from the hydrogen atoms of the methyl groups of **5**), using a riding model included in ShelX.[35] Hydrogen atoms were given isotropic thermal parameters 1.2 times the thermal parameter of the atoms to which they were attached. The water molecule hydrogen atoms could not be detected in **6**, also because they are necessarily (crystallographically) disordered about the 4-fold axis (as well as by the statistical mirror plane owned by the whole complex). In addition, the lack of suitable hydrophilic sites in the TPP periphery makes it likely that a dynamic reorientation of the H_2O molecule occurs. Selected details of the data collection and refinement are given in Table 1.

X-ray Powder Diffraction Studies. Purple powders **3** and **4** were gently ground in an agate mortar and then deposited in the hollow (0.1 mm deep) of a zero-background quartz monocrystal plate. Diffraction data (Cu Kα, $\lambda = 1.5418$ Å) were collected on a vertical scan θ:2θ Bruker D8 ADVANCE diffractometer,

(33) Sheldrick, G. M. (**1996**) *SADABS*, University of Göttingen, Göttingen, Germany (freely available on line at http://shelx.uni-ac.gwdg.de/axs/.

(34) Farrugia, L. J. *J. Appl. Crystallogr*. **1999**, *32*, 837−838.

(35) Sheldrick, G. M. *SHELX97: Programs for Crystal Structure Analysis*, release 97-2; Institüt für Anorganische Chemie der Universität: Göttingen, Germany, 1998.

equipped with parallel (Soller) slits, a secondary beam curved graphite monochromator, a Na(Tl)I scintillation detector, and pulse height amplifier discrimination. The generator was operated at 40 kV and 40 mA. The receiving slit was 0.2 mm. Nominal resolution for the present setup is 0.07° 2θ (fwhm) for the Si(111) peak at 28.44° (2θ). Long scans were performed with $5° < 2\theta < 80°$, $t =$ 30 s, and $\Delta 2\theta = 0.02°$ and used for structure solution and refinement.

Indexing, using TREOR,[36] of the low-angle diffraction peaks suggested tetragonal cells with the following approximate dimensions: $a = 13.41$ Å and $c = 9.73$ Å [$M(20) = 22$; $F(20) = 34$ (0.011, 54)] and $a = 13.24$ Å and $c = 19.44$ Å [$M(20) = 21$; $F(20) = 34$ (0.012, 52)] for **3** and **4**, respectively. Systematic absences indicated, among others, *I*4/*m* and *P*4/*nnc* as the probable space groups, later confirmed by successful solution and refinement. Structure solutions were initiated by the simulated annealing technique implemented in TOPAS,[37] using, as fragments, the metal atom and idealized pyrrolic and benzylic fragments. The final refinements were performed by the Rietveld method with the aid of TOPAS, with peak shapes described by the fundamental parameter approach and an isotropic crystal size broadening factor of Lorentzian contribution. The TPP fragments as a whole, lying on 4 or 4/*m* symmetry elements, have been eventually carefully modeled by constraining some of the rotational parameters of their constituents. A soft constraint was also given to the Ru−OH bond distance (2.10 Å) in **4**. The background function was modeled by a polynomial function, while further systematic errors were corrected with the aid of a sample displacement shift and a preferred orientation model (001 pole, in the March−Dollase formulation); a single isotropic displacement parameter was also refined. Scattering factors were taken from the internal library of TOPAS. Final agreement factors R_p, R_{wp}, and R_{Bragg} equaled 0.081, 0.112, and 0.038 for **3** and 0.086, 0.117, and 0.040 for **4**, respectively, for 3751 data points collected in the $5° < 2\theta < 80°$ range. Final Rietveld refinement plots are given in Figure 10. Eventually, species **3** and **4** were found to be isostructural with $[Ru^{IV}(TPP)(Br)_2]$[38] and $[Ru^{IV}(OEP)(OH)]_2O\cdot(CH_3OH)$,[16] respectively. A summary of the crystal data and refinement procedures can be found in Table 1. The structure of a similar species, namely, $Ti(TPP)Cl_2$, has been refined (not determined) by powder diffraction methods (using synchrotron radiation), taking the advantage of the already known fractional coordinates of the bromine derivative.[39]

Crystallographic data (excluding structure factors) for the structures reported in this paper have been deposited with the Cambridge Crystallographic Data Centre (Supplementary Publication CCDC 237680-237683). Copies of the data can be obtained free of charge on application to CCDC, 12 Union Road, Cambridge CB21EZ, U.K. [fax, (+44)1223-336-033; e-mail, deposit@ccdc.cam.ac.uk] or can be retrieved free of charge via www.ccdc.cam.ac.uk/conts/retrieving.html.

Conclusions

In this paper, we have reported a reproducible synthesis, in yield and purity, of $[Ru^{VI}(TPP)(O)_2]$ (**3**). Its molecular structure was determined by X-ray powder diffraction (XRPD) analysis. The solution behavior of **3** was investigated by NMR spectroscopy; PGSE measurements allowed us to identify the presence of two different solvates of **3** in the $CDCl_3$ solution. The reactivity of $[Ru^{VI}(TPP)(O)_2]$ was also investigated. It reacts in the presence of acids with $[Ru^{II}(TPP)(CO)]$ to yield $[Ru^{IV}(TPP)(OH)]_2O$, which can also be obtained by oxidation of $[Ru^{II}(TPP)(CO)]$ in CH_2Cl_2. Complex $[Ru^{IV}(TPP)(OH)]_2O$ was isolated in a polycrystalline form which allowed us to determine its molecular structure by XRPD. The reaction of $[Ru^{VI}(TPP)(O)_2]$ with DMSO and carbon monoxide gave $[Ru^{II}(TPP)(S\text{-}DMSO)_2]$ and $[Ru^{II}(TPP)(CO)(H_2O)]$, respectively. These complexes were completely characterized, including conventional single-crystal X-ray diffraction analysis. Moreover, the commonly employed Ru(TPP)(CO) has been shown to be a solid solution of authentic [Ru(TPP)(CO)] and $[Ru(TPP)(CO)(H_2O)]$ in variable proportions.

Acknowledgment. We thank MIUR (Programmi di Ricerca Scientifica di Rilevante Interesse Nazionale, PRIN 2003033857), the Fondazione Provinciale Comasca, and the University of Insubria (Progetto di Ateneo "Sistemi Poliazotati") for financial support. We are grateful to Mr. Pasquale Illiano (Dipartimento di Chimica Inorganica Metallorganica e Analitica, Università degli Studi di Milano) for performing PGSE analysis. N.M. and A.S. thank Dr. A. Kern (Bruker AXS, Karlsrube, Germany) for providing the β-version of TOPAS.

Supporting Information Available: X-ray data for **3**−**6**. This material is available free of charge via the Internet at http://pubs.acs.org.

IC048587W

(36) Werner, P. E.; Eriksson, L.; Westdahl, M. *J. Appl. Crystallogr*. **1985**, *18*, 367−370.
(37) *TOPAS*, version 3.1; Bruker AXS: Karlsrube, Germany, 2004.
(38) Ke, M.; Sishta, C.; James, B. R.; Dolphin, D.; Sparapany, J. W.; Ibers, J. A. *Inorg. Chem*. **1991**, *30*, 4766−4771.
(39) Christensen, A. N.; Grand, A.; Lehman, M. S.; Cox, D. E. *Acta Chem. Scand.* **1990**, *44*, 103−105.